

Characterization of Nanoaerosol Size Change During Enhanced Condensational Growth

P. Worth Longest, James T. McLeskey Jr. & Michael Hindle

To cite this article: P. Worth Longest, James T. McLeskey Jr. & Michael Hindle (2010) Characterization of Nanoaerosol Size Change During Enhanced Condensational Growth, *Aerosol Science and Technology*, 44:6, 473-483, DOI: [10.1080/02786821003749525](https://doi.org/10.1080/02786821003749525)

To link to this article: <https://doi.org/10.1080/02786821003749525>



Published online: 29 Apr 2010.



Submit your article to this journal [↗](#)



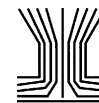
Article views: 1017



View related articles [↗](#)



Citing articles: 5 View citing articles [↗](#)



Characterization of Nanoaerosol Size Change During Enhanced Condensational Growth

P. Worth Longest,^{1,2} James T. McLeskey, Jr.,¹ and Michael Hindle²

¹Department of Mechanical Engineering, Virginia Commonwealth University, Richmond, Virginia, USA

²Department of Pharmaceutics, Virginia Commonwealth University, Richmond, Virginia, USA

Increasing the size of nanoaerosols may be beneficial in a number of applications, including filtration, particle size selection, and targeted respiratory drug delivery. A potential method to increase particle or droplet size is enhanced condensational growth (ECG), which involves combining the aerosol with saturated or supersaturated air. In this study, we characterize the ECG process in a model tubular geometry as a function of initial aerosol size (mean diameters—150, 560, and 900 nm) and relative humidity conditions using both *in vitro* experiments and numerical modeling. Relative humidities (99.8–104%) and temperatures (25–39°C) were evaluated that can safely be applied to either targeted respiratory drug delivery or personal aerosol filtration systems. For inlet saturated air temperatures above ambient conditions (30 and 39°C), the initial nanoaerosols grew to a size range of 1000–3000 nm (1–3 μm) over a time period of 0.2 s. The numerical model results were generally consistent with the experimental findings and predicted final to initial diameter ratios of up to 8 after 0.2 s of humidity exposure and 14 at 1 s. Based on these observations, a respiratory drug delivery approach is suggested in which nanoaerosols in the size range of 500 nm are delivered in conjunction with a saturated or supersaturated air stream. The initial nanoaerosol size will ensure minimal deposition and loss in the mouth-throat region while condensational growth in the respiratory tract can be used to ensure maximal lung retention and to potentially target the site of deposition.

INTRODUCTION

Although nanoaerosols are advantageous in many applications, their small size and increased reactivity also lead to toxicological concerns and difficulties with processing and handling (Hood 2004; Kreyling et al. 2004; Maynard et al. 2004; Oberdorster et al. 2004; Kreyling et al. 2006; Azarmi et al. 2008).

Received 16 October 2009; accepted 1 March 2010.

This study was supported by Award Number R21HL094991 from the National Heart, Lung, and Blood Institute. The content is solely the responsibility of the authors and does not necessarily represent the official views of the National Heart, Lung, and Blood Institute or the National Institutes of Health.

Address correspondence to P. Worth Longest, Virginia Commonwealth University, 401 West Main Street, P.O. Box 843015, Richmond, VA 23284-3015, USA. E-mail: pwlونغest@vcu.edu

Common pollutants such as diesel exhaust (5–500 nm) (Kittelson 1998) and cigarette smoke (20–1600 nm) (Bernstein 2004), as well as bioaerosols such as Avian flu and SARS (20–200 nm) (Mandell et al. 2004), are within the nanoaerosol range. An effective method for increasing the size of nanoaerosols may be beneficial in a number of applications, including particle removal, size selection, generation, and respiratory drug delivery. For example, filtration of aerosols in the range of 40–900 nm is difficult due to a lack of sufficient inertia and Brownian motion for efficient deposition (Brown 1993; Maze et al. 2007). Aerosols in this size range also typically have low electrical mobilities, making removal by electrostatic precipitation less effective (Hinds 1999; Tepper and Kessick 2008). Increasing the size of contaminant nanoaerosols could allow for increased inertial deposition, improving filter effectiveness without increasing pressure drops and flow rates. Larger aerosols may also hold more charge, thereby increasing their electrical mobility and the related effectiveness of electrostatic precipitators (Hinds 1999; Choi and Kim 2007). In other applications, increasing the size of nanoaerosols after a period of time or at a particular location may be advantageous. Size increase may be used to halt the columbic cascade of droplet explosions during electrospray aerosol generation after a certain period of time, allowing for better control of droplet size and contents. Considering inhaled therapeutic nanoaerosols, controlling the rate of size increase may be used to reduce mouth-throat deposition, ensure full lung retention, and potentially target the site of deposition (Longest et al. 2009).

Enhanced condensational growth (ECG) offers an effective method to significantly increase the size of nanoaerosols, potentially on a size selective basis. This process involves the combination of saturated or supersaturated water vapor (or other vapor species) with a nanoaerosol in a controlled manner. Under supersaturated conditions, the nanoparticles serve as heterogeneous nucleation sites and will grow in size due to water condensation (Friedlander et al. 1994; Hinds 1999). If saturated water vapor conditions are employed, then cooling is required to produce supersaturation, which can be accomplished by delivering the aerosol stream at a temperature below the humidity source temperature. Growth can also be obtained at saturated or

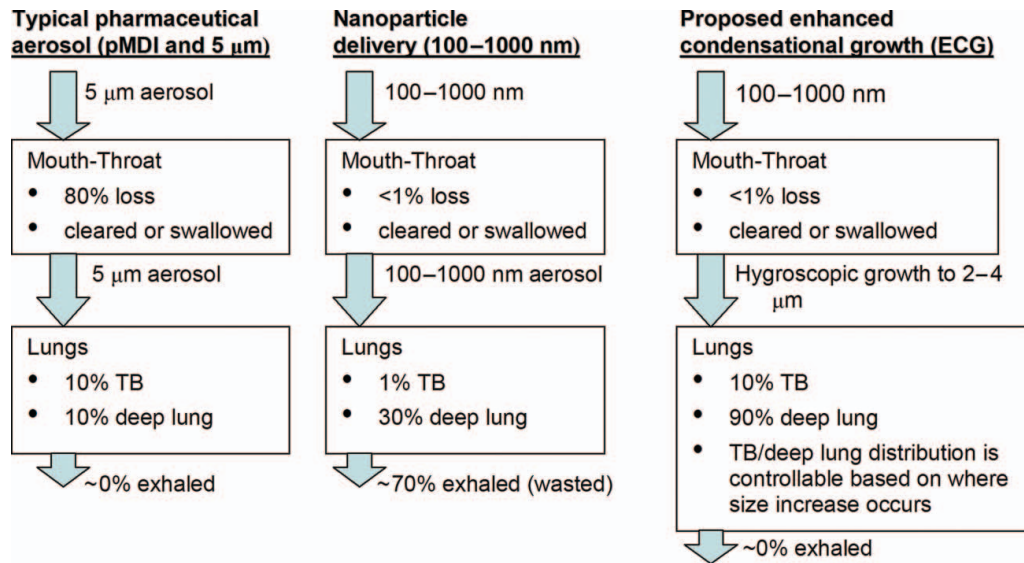


FIG. 1. Comparison of standard pressurized metered dose inhaler (pMDI) and nanoparticle delivery performance with the proposed enhanced condensational growth (ECG) approach. The standard and nanoparticle delivery methods either have high mouth throat (MT) deposition or allow a significant fraction of the aerosol to be exhaled. In contrast, the ECG approach offers both low MT deposition and full lung retention of the inhaled aerosol. Tracheobronchial (TB) versus alveolar deposition can potentially be engineered based on the rate of nanoparticle size increase.

subsaturated conditions if the nanoaerosol is hygroscopic (Hinds 1999). Relative humidities of water vapor can approach 400% before homogeneous nucleation starts to occur (Hinds 1999).

The enlargement of aerosols by condensational growth is the working principle behind condensational particle counters (CPCs), as reviewed by McMurry (2000). These and other aerosol measurement devices create a region of supersaturation through adiabatic expansion (Pollak 1959), mixing airstreams of different temperatures (Kousaka et al. 1982; Wang et al. 2002), or using a flow-through tube with a temperature different from the airstream (Stolzenburg and McMurry 1991; Hering and Stolzenburg 2005). Traditional CPCs typically used a cold-walled condenser approach with butanol or a similar gas as the condensing species (McMurry 2000). Hering and Stolzenburg (2005) developed the concept of a water-based condensation particle counter (WCPC) and used a heated and wetted growth tube design. This study formed the basis for the commercially available TSI 3785 WCPC, which was evaluated by Petaja et al. (2006), and subsequent WCPC models. Variations of the WCPC, such as a swirling flow design, have also been considered (Mordas et al. 2008). These previous studies provide a wealth of data on the growth of aerosols in supersaturated air fields. However, the effects of lower relative humidity values and biologically safe temperatures, which are more practical in personal aerosol filtration and respiratory drug delivery applications, on nanoaerosol size increase have not been previously investigated. Furthermore, the extent to which depletion of the water vapor by condensation onto the droplets (two-way coupling) (Finlay 1998) will limit size increase is not well understood for non-dilute concentrations of nanoaerosols.

As a specific application, the ECG approach can be applied to targeted respiratory drug delivery. Current pharmaceutical inhalers are designed to produce an aerosol with a mass median aerodynamic diameter (MMAD) of approximately 2–5 μm (Hindle 2004; Smaldone 2006; Longest et al. 2008). As shown in Figure 1, a significant problem for conventional systems is that, due to aerosol size, spray momentum, and inertia, significant aerosol drug deposition occurs in the mouth-throat (MT) region allowing little drug to enter the tracheobronchial (TB) and alveolar airways, where it is intended to deposit (Leach et al. 1998; Cheng et al. 2001; Borgstrom et al. 2006; Longest et al. 2008). Inhaled nanoparticles in the range of 40–900 nm offer the advantage of negligible deposition in the MT region (Cheng 2003; Xi and Longest 2008a). However, a significant limitation of this method is low TB (~1%) and alveolar (~30%) deposition leading to approximately 70% of the aerosol being exhaled and wasted (Stahlhofen et al. 1989; Cohen et al. 1990; Jaques and Kim 2000; Morawska et al. 2005). This is the primary reason why pharmaceutical nanoparticle aerosols have failed to realize their potential for inhaled drug delivery to the lungs.

Enhanced condensational growth for respiratory drug delivery is a newly proposed concept that is intended to combine the drug delivery advantages of both nanoparticles and micrometer aerosols. A nanoaerosol containing an active agent (drug or marker) is initially generated and inhaled past the MT resulting in low deposition and loss. The nanoaerosol is delivered with sufficient water vapor to cause supersaturation and aerosol growth to micrometer size in the TB and/or alveolar airways, which facilitates pulmonary retention. As a result, negligible

MT and near 100% lung deposition is possible. Furthermore, regional TB or alveolar deposition can be engineered allowing for drug targeting by controlling the rate of size increase. Factors affecting the rate of growth include the initial aerosol size, drug hygroscopicity, and the gas phase conditions of the humidity and aerosol delivery streams (i.e., temperature, relative humidity, and flow rate).

In this study, the ECG process is characterized in a model geometry for nanoaerosols with mean diameters of 150, 560, and 900 nm, using *in vitro* experiments and numerical modeling. Nanoparticles in this size range are difficult to filter and are a favorable initial dimension for ECG respiratory drug delivery. Ideally, a size increase of these aerosols to greater than 2 μm would allow for targeted respiratory deposition or a significant improvement in filtration efficiency, depending on the intended application. The experimental system consists of separate humidified air and aerosol inlets, a condensational growth zone, and a cascade impactor for outlet size assessments. The relative humidity (RH), temperature, and flow rate conditions considered are representative of both respiratory drug delivery and personal aerosol filtration systems. Exiting aerosol sizes as functions of initial size, RH, and temperature conditions are assessed based on both the *in vitro* experiments and numerical modeling. The numerical model is then used to further explore the potential for size increase over different timescales and at different RH conditions.

METHODS

Model Geometry

To evaluate the feasibility of ECG for respiratory drug delivery or personal aerosol filtration applications, a simple tubular geometry was selected as shown in Figure 2. At the geometry inlet, separate streams of humidified air and nebulized aerosol

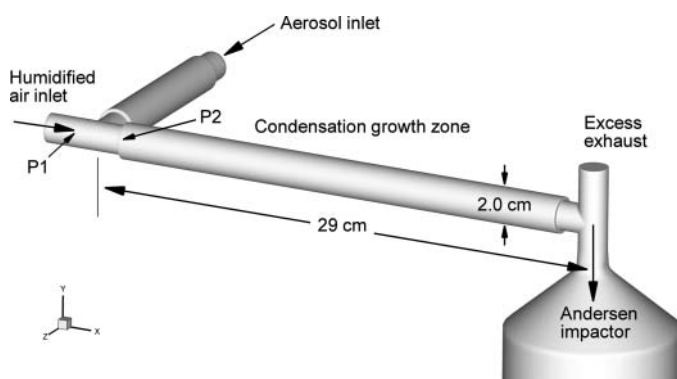


FIG. 2. A model of the *in vitro* geometry used to evaluate the ECG of submicrometer aerosols. The condensation growth zone was 29 cm in length, which is the approximate distance from the mouth to the main bronchi. Mixing of the aerosol stream with the heated and humidified air produces supersaturation conditions and aerosol growth. Final aerosol mass median aerodynamic diameters (MMAD) were determined with an Andersen cascade impactor (ACI) at the end of the condensation growth zone.

droplets are combined. The humidified air stream enters at a relative humidity (RH) of 100%, and the amount of entering water vapor is controlled based on the inlet temperature. The aerosol enters as submicrometer droplets or particles with a relatively monodisperse distribution. The temperature of the aerosol stream is below the temperature of the humidified air, resulting in supersaturated conditions when these two streams are mixed. The combined humidified air and submicrometer aerosol then enter a condensational growth zone with a length of 29 cm and a diameter of 2 cm. The length of the condensational growth zone is consistent with the distance from the mouth inlet to the first respiratory bifurcation in an adult male. The diameter of the growth zone provides a residence time that is approximately equal to the time required for an inhaled particle to reach the first respiratory bifurcation (i.e., about 0.2 s). As a result, the first mixing tee can be considered a first generation mouthpiece in a respiratory drug delivery application of ECG. Alternatively, the condensational growth zone is sufficiently short to be included in a personal aerosol filtration system. At the outlet of the condensational growth zone, a second connection tee is used to route the aerosol for size evaluation in the Andersen cascade impactor (ACI). For the tubular system of interest, the Reynolds number range is 500–2170, based on flow rates of 7.5–32.5 L/min (Table 1) and a 2 cm inner diameter. Considering the presence of 90° bends and the combination of two flow streams, laminar through mildly turbulent flow conditions are expected for this range of Reynolds numbers.

Aerosol Generation and Delivery

Nano-sized aqueous-based drug aerosols were generated using a small particle aerosol generator (SPAG- 6000, ICN Pharmaceuticals, Costa Mesa, CA). Albuterol sulfate solutions were nebulized using a series of nebulizer airflow conditions to produce aerosols with initial mean (SD) measured sizes of 150 (5.5) nm, 560 (11.4) nm, and 900 (32.7) nm, respectively (Table 1). The 150 nm aerosol was generated using a 0.1% albuterol sulfate in water solution and exited the SPAG with a flow rate of 15 L/min. For the 150 nm aerosol, the flow delivered to the condensational growth tube was reduced to 7.5 L/min, using a negative pressure line, thus diluting the delivered aerosol. The 560 nm aerosol was generated using a 0.1% albuterol sulfate in water solution at a total flow rate of 9.0 L/min. The 900 nm aerosol was generated using a 0.5% albuterol sulfate in water solution and was also delivered at a flow rate of 9.0 L/min. Aerosols were generated for 5, 2.5, and 1 min, respectively, for the 150, 560, and 900 nm sizes. Aerosols exiting the SPAG drying chamber were then mixed with the humidified air and entered the 29 cm condensation growth tube as shown in the schematic diagram of the experimental setup in Figure 2.

A modified compressed-air-driven humidifier system (VapoTherm 2000i, Stevensville, MD) was employed to generate heated saturated and supersaturated air conditions flowing through the tubular geometry at 20 L/min (25 L/min was

TABLE 1
Experimental flow conditions

	Aerosol inlet	Humidified air inlet	Impactor (ACI) inlet ^c
150 nm	<i>Q</i> : 15 L/min (250 cm ³ /s) ^a <i>T</i> : 20°C <i>RH</i> : 82.5%	<i>Q</i> : 25 L/min (416.7 cm ³ /s) <i>T</i> : 25, 30, and 39°C <i>RH</i> : 100% <i>n</i> ^b : ~ 0 part/cm ³	<i>Q</i> : 32.5 L/min (541.7 cm ³ /s) <i>n</i> : 6.0 × 10 ⁴ part/cm ³
560 nm	<i>Q</i> : 9.0 L/min (150 cm ³ /s) <i>T</i> : 21°C <i>RH</i> : 97.5%	<i>Q</i> : 20 L/min (333.3 cm ³ /s) <i>T</i> : 25, 30, and 39°C <i>RH</i> : 100% <i>n</i> : ~ 0 part/cm ³	<i>Q</i> : 29.0 L/min (483.3 cm ³ /s) <i>n</i> : 1.2 × 10 ⁵ part/cm ³
900 nm	<i>Q</i> : 9.0 L/min (150 cm ³ /s) <i>T</i> : 21°C <i>RH</i> : 97.5%	<i>Q</i> : 20 L/min (333.3 cm ³ /s) <i>T</i> : 25, 30, and 39°C <i>RH</i> : 100% <i>n</i> : ~ 0 part/cm ³	<i>Q</i> : 29.0 L/min (483.3 cm ³ /s) <i>n</i> : 2.8 × 10 ⁵ part/cm ³

^aThe flow rate of the aerosol inlet was reduced to 7.5 L/min for the 150 nm case prior to entering the condensation growth tube.

^bAmbient particle concentration was approximately <100 particle/cm³ and considered negligible.

^cAll flow exited through the ACI.

employed for the 150 nm aerosol). As shown in Table 1, the humidified air enters the mixing tee with a relative humidity (RH) of 100% and temperatures of 25, 30, and 39°C. Each successive increase in temperature holds more water vapor mass at a RH of 100%. Therefore, mixing with the 20–21°C aerosol stream is intended to create a higher degree of supersaturation for each increase in humidified air temperature. The condensation tube and impactor were maintained at a constant temperature inside an environmental cabinet (Espec Environmental Cabinet, Grand Rapids, MI) corresponding to the temperature of the incoming aerosol mixture (measured at P2 in Figure 2, as determined below). The temperature of the humidified air / aerosol mixture was measured independently for each set of experimental conditions prior to the final growth experiments. Following passage through the condensational growth tube, aerosols were delivered to the ACI (Graseby-Andersen Inc, Smyrna, GA) for particle sizing. The aerosol particle concentration was also determined at the entrance to the cascade impactor, using a condensation particle counter (CPC 3022A, TSI Inc, Shoreview, MN) sampling at 25 cm³/s.

In separate experiments for each of the cases considered in Table 1, the temperature and humidity of the humidified air and aerosol mixture streams at the inlet to the condensational growth tube were measured. These measurements were performed using the Humicap Handheld Meter (HMP75B, Vaisala, Helsinki, Finland) positioned at the mid-plane of the tubing (P1 on Figure 2) and a sheathed Type K thermocouple (Omega Engineering Corp., Stamford, CT) positioned at the mid-plane of the tubing (P2 on Figure 2), respectively. The Humicap Handheld Meter has a stated temperature accuracy of ±0.2°C (at 20°C) and ±0.25°C (at 40°C). It has a RH accuracy of ±1.7% (at 20°C) and ±1.8% (at 40°C) between 90–100% RH. The probe was factory calibrated using traceable standards and supplied with a NIST calibration certificate. The probe was housed in a plastic filter and incorporated a sensor pre-heater, which was employed

to prevent condensation during equilibration prior to measurement and had a response time of 17 s in still air. In all cases, experimental duration (>30 s) was sufficient to allow equilibration of the probes. Particle sizing of these aerosols was not performed during temperature and humidity measurements due to possible drug deposition on the probes altering the measured distribution.

Analysis of Initial and Final Droplet Sizes

The initial aerodynamic particle size distribution of the aerosol exiting the SPAG drying chamber was determined using the 10 stage MOUDI operated at 30 ± 2 L/min (MSP Corp, Shoreview, MN), which allowed size fractionation between 50 nm and 10 μm. Humidified co-flow air (99% RH) was supplied to the impactor, which was placed in the environmental chamber and held at constant temperature and humidity conditions of 25°C and 99% RH. The final aerodynamic particle size distribution of the aerosol exiting the condensational growth tube was determined using the ACI operated at 28.3 ± 2 L/min. The ACI is preferable for the larger particle sizes observed following condensational growth. Similarly, the impactor was placed in the environmental chamber and held at constant temperature conditions (as previously described) and at a relative humidity of 99%. For both the initial and final particle size distributions, following aerosol generation, washings were collected from the impaction plates to determine the drug deposition. A 1:1 admixture (25 mL total) of methanol and de-ionized water was used, and the solutions were then assayed using a validated HPLC-UV method for albuterol sulfate. The mass of drug on each impaction plate was determined and used to calculate both the initial and final aerodynamic particle size distributions of the drug aerosols. Aerosol droplet size distributions were reported as albuterol sulfate mass distribution recovered from the impactor. The mass median aerodynamic diameter (MMAD)

was defined as the particle size at the 50th percentile on a cumulative percent mass undersize distribution (D50) using linear interpolation. Five replicates of each experiment were performed. Statistical comparisons were made using a paired t-test, comparing the initial MMAD with that obtained following exposure to enhanced condensational growth conditions. Significance was assessed at $P < 0.01$ using a two-tailed test.

Numerical Model of Droplet Size Change

A numerical model of evaporation and condensation for a single droplet was developed, based on the governing equations of heat and mass conservation (Ferron 1977; Hinds 1999). Coupling between the heat and mass transport was included such that droplet temperature increased during condensation due to the latent heat of water vapor. A rapid mixing model (RMM) approach was employed, which assumes that concentrations and temperatures within the droplet are constant with negligible gradients compared with much larger gradients outside of the droplet. The RMM approach was previously validated for application to respiratory aerosols by Longest and Kleinstreuer (2005). The governing differential equations for multi-component droplet evaporation and condensation used in this study were reported in detail by Longest and Xi (2008).

Non-continuum effects on the heat and mass transfer of the nanoaerosol were accounted for using the Knudsen correlations given by Fuchs and Sutugin (1970) and Finlay (2001). The temperature-dependent saturation pressure of water vapor on the droplet surface was determined from the Antoine equation. This saturation pressure was modified for hygroscopic effects with an experimentally determined activity coefficient for albuterol sulfate. Individual activity coefficients were measured for albuterol sulfate mass fractions ranging from 0.005 to 0.28. The resulting data was fit to a multi-component form of Raoult's law (Hinds 1999), resulting in a van't Hoff factor of $i = 0.865$. The influence of the Kelvin effect on droplet surface concentrations of water vapor was also included, which increases as droplet size decreases below approximately $1 \mu\text{m}$. The resulting increase in surface vapor pressure will reduce the potential for condensation and increase the potential for evaporation at a given RH condition. As a result, condensation may not occur or may be reduced as a function of droplet size even for supersaturated relative humidity conditions. Based on particle size, slip velocities were neglected and the Nusselt and Sherwood numbers were approximated with diffusional estimates (Clift et al. 1978). The resulting coupled governing equations for droplet heat and mass transfer were solved using a variable time-step accuracy-controlled coupled differential equation solver in the numerical package MathCAD 13 (Mathsoft Apps.). Reducing the accuracy control limit by an order of magnitude had a negligible (less than 1%) effect on the final predicted aerosol diameters.

RESULTS

In Vitro Evaluation of Aerosol Growth

Relatively monodisperse nanoaerosols from an albuterol sulfate solution (0.1% or 0.5% w/v) were generated using the SPAG. In addition to particle size, humidified air and aerosol inlet conditions were adjusted as specified in Table 1. Initial drug aerosol particle size distributions were determined as the aerosol exited the SPAG drying tube with MMADs and standard deviations (SD) shown in Table 2. Final drug aerosol MMADs following passage through the condensation growth tube were similarly determined and are also shown in Table 2, along with SD values, based on a minimum of five replicates. In each case, the humidified inlet air was at saturated conditions ($\text{RH} = 100\% \pm 1.8\%$). For a saturated air inlet temperature of 25°C , significant size change is observed with the 150 nm aerosol ($P < 0.01$ paired t-test), but diminishing changes occur for the 560 and 900 nm droplets (Table 2; $P > 0.01$ paired t-test). Considering a humidified air inlet temperature of 30°C , significant size increases are observed for each of the three initial aerosol diameters measured. At this temperature, all three size groups increase to 1000 nm ($1.0 \mu\text{m}$) or above, which can significantly improve filtering efficiency. In addition, the initially 560 and 900 nm droplets increase in diameter to above 2000 nm ($2 \mu\text{m}$), which will improve lung retention to near 100% (Heyder et al. 1986; Stahlhofen et al. 1989) and can potentially be used for targeted lung deposition. Increasing the air inlet temperature to 39°C results in more available water mass for condensation and further increases in aerosol growth. However, the percentage of size increase associated with increasing the temperature from 30 to 39°C is relatively small, compared with the previous temperature increase. This diminished return on final aerosol size, as temperature is increased, may be due to either (i) an increased loss of water mass on the tube walls due to higher RH values or (ii) a limit in particle size increase resulting from the available amount of water vapor.

Considering the effect of initial size, a significant increase in final diameter is associated with increasing the original size

TABLE 2

Final droplet mass median aerodynamic diameter (MMAD) based on the *in vitro* ACI measurements. Standard deviation values based on a minimum of five replicates for each case are reported in parentheses. Estimated initial mass fractions of albuterol sulfate in the 150, 560, and 900 nm droplets were 100%, 31%, and 49%, respectively

Initial size	Final MMAD at specified inlet temperature		
	25°C	30°C	39°C
150 nm (5.5)	432 nm* (54)	988 nm* (58)	1228 nm* (79)
560 nm (11.4)	610 nm (37)	2256 nm* (168)	2664 nm* (129)
900 nm (32.7)	1158 nm (145)	2240 nm* (116)	2630 nm* (86)

* $P < 0.01$ paired t-test compared to initial size.

TABLE 3

Numerical predictions of final aerosol size and potential for two-way coupling during aerosol growth. Based on the experiments, the numerical model assumed the initial mass fractions of albuterol sulfate in the 150, 560, and 900 nm aerosols were 100%, 31%, and 49%, respectively

Initial aerosol size (nm)	Humidified air inlet temp. (°C)	Numerical prediction of final aerosol size (nm)	Percent error for predicted size (%)	ζ (Significant growth if $\zeta \geq 0.3$) ^a	γ (Two way coupling if $\gamma \geq 0.1$) ^b
150	25	160	63	30287	1.3E-6
	30	180	82	28196	1.5E-6
	39	1290	5	71	6.7E-3
560	25	880	44	37	0.027
	30	1620	28	13	0.15 ^c
	39	3120	17	18	0.21 ^c
900	25	1510	30	21	0.12 ^c
	30	2040	9	12	0.30 ^c
	39	3330	26	16	0.40 ^c

^aImportance of size change if the aerosol were treated as a single droplet (Finlay 1998).

^bMass of droplets divided by mass of vapor per unit volume (Finlay 1998).

^cTwo-way coupling predicted based on γ greater than or equal to approximately 0.1.

from 150 to 560 nm (Table 2). In contrast, the final aerosol size is similar between the 560 and 900 nm initial diameter cases for each of the three inlet temperatures. The Kelvin effect, which increases the partial pressure of water vapor on the surface of nanodroplets as the size is reduced (Finlay 2001), may be a limiting factor in the amount of size increase associated with the 150 nm aerosol. However, for larger initial particles (560 and 900 nm), the ECG process appears to produce final aerosol diameters that are not highly dependent on the initial size for each inlet temperature condition.

Numerical Predictions of Aerosol Growth

Bulk temperature and relative humidity conditions were estimated as mass-flow-rate-weighted averages of the aerosol and humidified air inlet conditions (Table 1). This approach assumes that the aerosol and humidified streams are fully mixed at the start of the condensational growth zone. The resulting relative humidity conditions for saturated air inlet temperatures of 25, 30, and 39°C were approximately 99.8, 101, and 104%, respectively. The numerical model accounted for the Kelvin and Fuchs effects, the concentration dependent activity coefficients, and the coupling between droplet heat and mass transfer. However, condensation growth in this model was not limited by depletion of the water-vapor in the continuous phase (i.e., the bulk temperature and humidity were held constant). Numerical predictions of final droplet size based on a calculated residence time in the condensation growth zone of 0.17–0.19 s (Table 1) are presented in Table 3, along with percent errors in comparison with the *in vitro* results. Relative percent errors are calculated as

$$\frac{|\text{experimental value} - \text{numerical value}|}{\text{experimental value}} \times 100. \quad [1]$$

The model predictions are in agreement with the *in vitro* measurements in some cases, with relative percent errors below 5%. However, the model predictions do not agree with the experiments in other cases, with a maximum error of approximately 80%. In general, the model results under predict the growth of the initial 150 nm aerosol and over predict the growth of the 560 and 900 nm droplets. Initial mass fractions of albuterol sulfate in the 150, 560, and 900 nm droplets were estimated to be 100%, 31%, and 49%, respectively. Under prediction of the 150 nm, aerosol final size may be associated with limitations in the correlation used to predict the surface activity coefficient at high mass fractions of albuterol sulfate. For the initially larger sizes, over predictions of the final MMAD, in some cases, may be due to depletion of the water vapor available for continued growth. This, and other factors, are not considered in the model. The effect of size change in the droplet phase on the amount of available water vapor is referred to as two-way coupling.

In order to evaluate the effects of two-way coupling on the final droplet size, the analytical analysis of Finlay (1998) was applied. Briefly, Finlay (1998) defined the non-dimensional number ζ as the ratio of added mass to existing droplet mass, which is large (>0.3) if the size change is significant. A second parameter, γ , represents the ratio of particle mass to the mass available for condensation until equilibrium is reached. A value of γ greater than approximately 0.1 indicates that two-way coupling is significant, and a value greater than approximately 3.0 indicates that condensational growth is not possible due to high aerosol concentrations. Considering these non-dimensional parameters applied to the initial aerosol sizes (150, 560, and 900 nm), growth is expected to be significant, and two-way coupling is not expected. In Table 3, ζ and γ values are reported based on the final predicted droplet sizes and experimentally determined outlet number concentrations of 6×10^4 , 1.2×10^5 , and $2.8 \times$

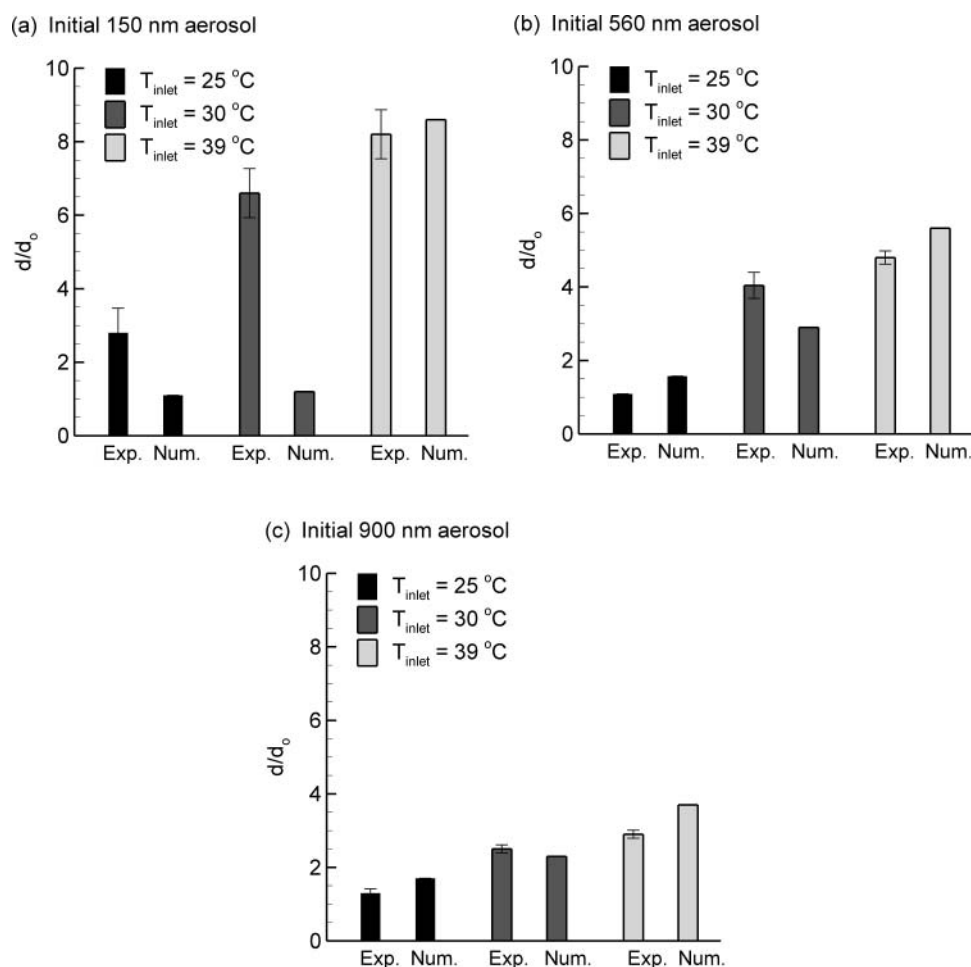


FIG. 3. Comparison of experimental measurements and numerically predicted growth ratios of final to initial aerosol diameters (d/d_0) at three humidified air inlet temperatures for initial sizes of (a) 150 nm, (b) 560 nm, and (c) 900 nm with initial albuterol sulfate mass fractions of 100%, 31%, and 49%, respectively. *In vitro* error bars represent \pm one standard deviation (SD) of the experimental data. Inaccuracies in the numerical predictions for the 150 nm aerosol case may be due to limitations of the correlation used to predict the surface activity coefficient at higher mass fractions of drug. For most other cases, the numerical model provides a reasonable estimate of the growth ratio.

10^5 part/cm³ for the 150, 560, and 900 nm aerosols, respectively. Considering the ζ parameter, size change is expected to be large for all cases. However, the mass of available water vapor (γ) indicates that two-way coupling may occur for the two larger aerosol sizes evaluated at most inlet temperatures. Moreover, the coupling is expected to be strongest for the cases with the largest final size (i.e., initial diameters of 560 and 900 nm and an inlet temperature of 39°C).

Although γ values above 0.1 are observed for the two larger aerosol sizes, two-way coupling cannot fully explain the observed differences between the numerical predictions and experimental results. If two-way coupling was the primary factor controlling these differences, then the model should over predict growth in all cases in a manner proportional to the size of γ . Comparisons between Tables 2 and 3 indicate that this is not the case. Specifically, at 30°C, the growth of the two larger aerosol sizes (560 and 900 nm) is under predicted. In contrast, at 39°C, the numerical model over predicts the final aerosol size, which

is consistent with two-way coupling. This data suggests that multiple factors, in addition to two-way coupling, may produce differences between the experimental and modeling results. Additional factors that may influence the rate of growth include: loss of water vapor on the growth tube wall, incomplete mixing, and experimental uncertainties in the temperature and humidity measurements. Two-way coupling is most likely to have a mild to moderate influence on the growth, which is strongest for the larger aerosols and higher temperatures (i.e., larger γ values) considered.

A comparison of experimentally determined and numerically predicted final to initial diameter growth ratios (d/d_0) is presented in Figure 3. The numerical model provides a reasonable approximation of the experimentally observed growth ratios. However, large differences remain between the numerical predictions and experimental data for the initial 150 nm size at inlet temperatures of 25 and 30°C. As indicated, this may be the result of limited activity coefficient data for highly concentrated

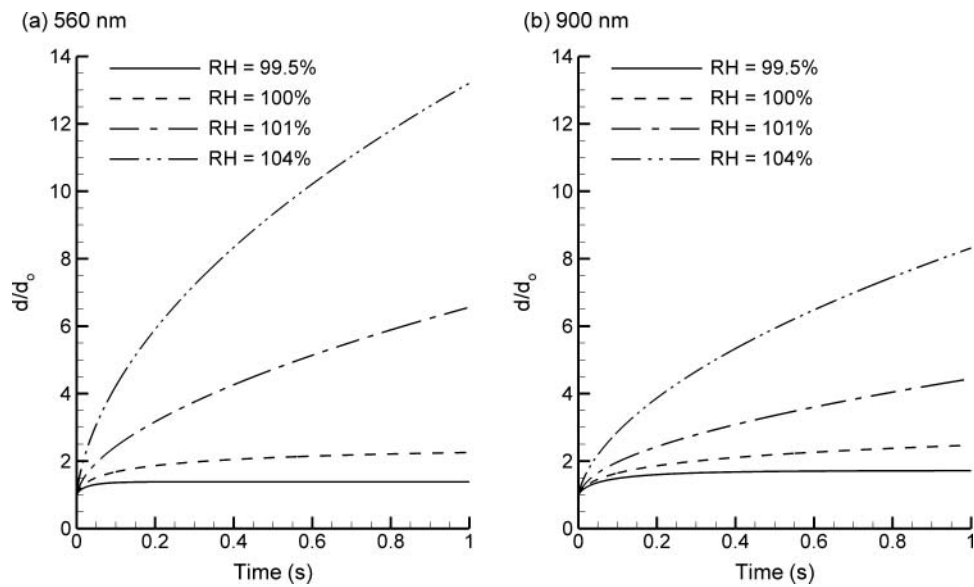


FIG. 4. Numerical predictions of growth ratios (d/d_0) over a 1 s period for a range of RH values (99.5–104%), body temperature conditions ($T_{\text{body}} = 37^\circ\text{C}$), and initial aerosol sizes of (a) 560 nm and (b) 900 nm. Relatively minor changes in the RH condition result in large changes in the rate of aerosol growth and the final size achieved. As a result, ECG appears to be an effective method for changing the size of an aerosol after inhalation, thereby nearly eliminating mouth-throat deposition and ensuring full lung retention.

albuterol sulfate aerosols. Considering the cases where coupling is expected (the 560 nm aerosol with $T_{\text{inlet}} = 39^\circ\text{C}$ and the 900 nm aerosol with $T_{\text{inlet}} = 30$ and 39°C), relatively little difference is observed between the numerical model predictions and the experimental data. As a result, it is concluded that two-way coupling (which is absent in the numerical model) does not significantly limit particle growth in the system of interest. Based on the percent errors reported in Table 3, this limitation appears to be 30% or less. Growth ratios are largest for the highest inlet temperature considered $T_{\text{inlet}} = 39^\circ\text{C}$. Under this condition, the growth ratios for the 150, 560, and 900 nm initial aerosol sizes are approximately 8, 4, and 3, respectively.

Potential for Continued Aerosol Growth

An advantage of the numerical model is that conditions can be adjusted to predict growth under different scenarios. The effect of RH on aerosol growth at a bulk air temperature of 37°C , consistent with the temperature of the respiratory airways, for two initial aerosol sizes is shown in Figure 4. The time interval for aerosol growth has been extended from the residence time in the *in vitro* model (approximately 0.17–0.19 s) to an approximate time period of one inhalation cycle (approximately 1 s). Considering the unaltered relative humidity of the respiratory tract to be 99.5% (Ferron 1977), little growth is observed, which arises from hygroscopic effects of the dissolved albuterol sulfate. In contrast, saturated and supersaturated conditions, up to a RH of 104%, result in growth ratios that range from approximately 2 to 14 for the 560 nm aerosol and 2 to 8 for the 900 nm aerosol. These values are expected to be overestimates of actual growth due to the omission of both two-way coupling effects and

vapor loss on the tube wall or in the respiratory tract. However, these estimates indicate the approximate scale and time history of growth that can be obtained within the time period of one respiratory inhalation cycle. Furthermore, these values become more accurate for decreased aerosol number concentrations, as with environmental aerosols or therapeutic aerosols delivered over a longer exposure period.

DISCUSSION

In this study, the effects of initial nanoaerosol size and inlet conditions on condensational aerosol growth were evaluated for temperatures and humidities appropriate for efficient low-power aerosol filtration or respiratory drug delivery. Factors limiting aerosol growth were identified as the residence time in the condensation growth zone, the Kelvin effect, two-way coupling, and some condensation adhering to the growth tube walls. Still, significant growth was observed for the initial nanoaerosol droplets and the relatively low temperatures considered. Growth above 1000 nm occurred for a saturated inlet temperature of 30°C and all initial aerosol sizes. Growth near 3000 nm was observed in some cases for an inlet temperature of 39°C , which is only 2°C above standard body temperature. As a result, ECG appears feasible for targeted respiratory drug delivery and as a method to significantly improve the filtration of nanoaerosols without increasing pressure losses. Interestingly, the two larger initial aerosol sizes grew to similar mean diameters for each inlet temperature considered. It can be concluded that above a certain lower size limit, the ECG process will result in a larger aerosol with a mean size controlled by the applied temperature and humidity conditions. The lower size limit, below which aerosols

undergo reduced growth, may be controlled by the Kelvin effect, applied temperature and RH conditions, and available exposure time.

The results of this study indicate that ECG, at the relatively low temperatures and humidities considered, may significantly improve respiratory drug delivery of nanoparticle aerosols, the therapeutic potential of which has yet to be fully realized. The initial aerosol sizes considered in this study are known to have negligible deposition in the MT and in a more general extrathoracic region that includes the nasal airways (Cheng 2003; Xi and Longest 2008a; Xi and Longest 2008b). Borgstrom et al. (2006) reported that in addition to minimizing drug loss and side effects, reduced MT deposition can significantly reduce variability in lung deposition, making inter- and intra-subject dosing more consistent. As shown in Longest and Xi (2008), the inhalation of saturated air several degrees above body temperature can increase the RH of the airways to supersaturated conditions. Furthermore, the generation and delivery of a warm saturated airstream is not technically challenging (Larsson et al. 2000) and not harmful to the patient (Branson et al. 1993). Increasing the size of respiratory aerosols to $2\ \mu\text{m}$ and above will ensure lung deposition in most cases (Stahlhofen et al. 1989).

A primary concern with the enhanced condensational growth approach applied to respiratory drug delivery is that aerosol number concentration will significantly limit size growth due to two-way coupling. The numerical model results of this study indicate that two-way coupling may be a factor even in the growth of nanoaerosols. Nevertheless, the desired size increases for effective respiratory drug delivery were observed both experimentally and numerically at concentrations consistent with clinical aerosol generation systems ($1 - 5 \times 10^5\ \text{part}/\text{cm}^3$). Large aerosol growth ratios, like those illustrated in Figure 4, can potentially be used to target deposition to specific regions of the lungs. However, lower particle concentrations and higher RH values than those used in the *in vitro* experiments may be required to achieve the growth ratios reported over 1 s in Figure 4. Based on these findings, further development and optimization of the ECG respiratory drug delivery concept will include evaluation in a more complex respiratory geometry, optimization for *in vivo* airways and boundary conditions, and animal model testing.

The simple model of droplet growth employed in this study provided a reasonable estimate of the trend in size increase. Considering the 150 nm aerosol, differences between model predictions and experimental results are most likely due to limitations in the correlation used to predict the surface activity coefficient at high mass fractions of albuterol sulfate. For the 560 and 900 nm cases, nondimensional analysis indicates that two-way coupling may be partially responsible for over predictions of aerosol size in some cases. However, other factors not included in the model, as well as experimental uncertainties, are also likely responsible for differences between the experimental results and numerical calculations. Considering the experiments, accurate humidity measurements near 100% are known to be difficult with an expected inaccuracy of $\pm 1.8\%$ for the

instrument that was used. Factors not considered in the numerical model include incomplete mixing of the airstreams, some loss of water vapor on the growth tube walls, and thermal coupling. The experimental geometry employed a standard mixing tee design (Figure 2) and had a maximum Reynolds number of 2170, indicating some transition to turbulence near the mixing region with likely relaminarization through the tube. However, this un-optimized combination of the flow streams and primarily laminar conditions likely result in incomplete mixing of the humidified air and aerosol. Therefore, the bulk fully mixed properties used in the simple isolated droplet model may have been inaccurate for predicting total growth compared with the experiments. Furthermore, incomplete mixing means that a temperature gradient exists across the flow field and across the tube wall. In the experiments, the measured centerline temperature at the mixing tee outlet was used to set the temperature of the cabinet and control the wall conditions. However, local differences from this centerline temperature, due to incomplete mixing, resulted in some condensation onto the walls of the growth tube. This loss of vapor mass reduced the experimentally observed outlet aerosol size. Finally, the two-way coupling analysis only considered the effect of available vapor mass. Thermal two-way coupling can also occur, in which condensation onto the aerosol increases the bulk air temperature, thereby reducing the relative humidity and potential for further condensation. Based on the simple one-dimensional droplet model employed in this study, it is not practical to isolate the relative contributions of each of these factors. Instead, further investigation of this system, using a computational fluid dynamics (CFD) approach that can resolve airstream mixing, turbulence, wall conditions, and mass/thermal two-way coupling is needed.

In addition to enhanced respiratory drug delivery, results of this study illustrate the potential of ECG for improving filtering efficiency and developing systems for the sorting and separation of nanoaerosols at relatively low temperatures and supersaturation values. As discussed, increasing the size of nanoaerosols to above $1\ \mu\text{m}$ can greatly improve filtering effectiveness without increasing flow rates and pressure losses. This concept has previously been suggested to improve the performance of wet scrubbers and impactors, using high temperature steam injection or large temperature differences on the order of 40°C or more (Lui et al. 1993; Sun et al. 1994; Sioutas and Koutrakis 1996). However, the current study is the first to illustrate the growth of nanoaerosols at relatively low temperature differences, which require less energy to improve filtration and for temperatures that can be tolerated for direct inhalation. Considering the separation of nanoaerosols from a polydisperse distribution, the ECG approach can be used to increase the size of droplets above what appears to be a Kelvin limit. These larger micrometer aerosols can then be easily filtered and removed using conventional impaction, leaving only the nanoaerosol fraction. The Kelvin limit, below which size increase is diminished, can be controlled as a function of the condensing vapor species surface tension, RH conditions, and exposure time. Further numerical and

experimental studies are needed to better develop the ECG process for improved particle removal, particle sorting, and other applications. However, results of the current study indicate that the ECG process is an effective mechanism for significantly increasing the size of nanoaerosols at relatively low temperatures and realistic particle concentrations that can be applied when nanoaerosol size is either detrimental or when droplet size needs to be modified as a function of time or location.

REFERENCES

- Azarmi, S., Roa, W. H., and Lobenberg, R. (2008). Targeted Delivery of Nanoparticles for the Treatment of Lung Diseases. *Adv. Drug Deliv. Rev.* 60:863–875.
- Bernstein, G. M. (2004). A Review of the Influence of Particle Size, Puff Volume, and Inhalation Pattern on the Deposition of Cigarette Smoke Particles in the Respiratory Tract. *Inhal. Toxicol.* 16:675–689.
- Borgstrom, L., Olsson, B., and Thorsson, L. (2006). Degree of Throat Deposition can Explain the Variability in Lung Deposition of Inhaled Drugs. *J. Aerosol Med.* 19:473–483.
- Branson, R. D., Davis, K., and Campbell, R. S. (1993). Humidification in the Intensive Care Unit. Prospective Study of a New Protocol Utilizing Heated Humidification and a Hygroscopic Condenser Device. *Chest.* 104:1800–1805.
- Brown, R. C. (1993). *Air Filtration: An Integrated Approach to the Theory and Applications of Fibrous Filters*. Pergamon, Oxford, U.K.
- Cheng, Y. S. (2003). Aerosol Deposition in the Extrathoracic Region. *Aerosol Sci. Technol.* 37:659–671.
- Cheng, Y. S., Fu, C. S., Yazzie, D., and Zhou, Y. (2001). Respiratory Deposition Patterns of Salbutamol pMDI with CFC and HFA-134a Formulations in a Human Airway Replica. *J. Aerosol Med.* 14(2):255–266.
- Choi, Y., and Kim, S. (2007). An Improved Method for Charging Submicron and Nano Particles with Uniform Charging Performance. *Aerosol Sci. Technol.* 41:259–265.
- Clift, R., Grace, J. R., and Weber, M. E. (1978). *Bubbles, Drops, and Particles*. Academic Press, New York.
- Cohen, B. S., Sussman, R. G., and Lippmann, M. (1990). Ultrafine Particle Deposition in a Human Tracheobronchial Cast. *Aerosol Sci. Technol.* 12:1082–1093.
- Ferron, G. A. (1977). The Size of Soluble Aerosol Particles as a Function of the Humidity of the Air: Application to the Human Respiratory Tract. *J. Aerosol Sci.* 3:251–267.
- Finlay, W. H. (1998). Estimating the Type of Hygroscopic Behavior Exhibited by Aqueous Droplets. *J. Aerosol Med.* 11(4):221–229.
- Finlay, W. H. (2001). *The Mechanics of Inhaled Pharmaceutical Aerosols*, Academic Press, San Diego.
- Friedlander, S. K., Windeler, R. S., and Weber, A. P. (1994). Ultrafine Particle Formation by Aerosol Processes in Turbulent Jets: Mechanisms and Scale-Up. *NanoStruct. Mat.* 4:521–528.
- Fuchs, N. A., and Sutugin, A. G. (1970). *Highly Dispersed Aerosols*, Ann Arbor Science, Ann Arbor, MI.
- Hering, S., and Stolzenburg, M. R. (2005). A Method for Particle Size Amplification by Water Condensation in a Laminar, Thermally Diffusive Flow. *Aerosol Sci. Technol.* 39:428–436.
- Heyder, J., Gebhart, J., Rudolf, G., Schiller, C. F., and Stahlhofen, W. (1986). Deposition of Particles in the Human Respiratory Tract in the Size Range of 0.005–15 Microns. *J. Aerosol Sci.* 17(5):811–825.
- Hindle, M. (2004). Soft Mist Inhalers: A Review of Current Technology. *The Drug Delivery Companies Report*. Autumn/Winter:31–34.
- Hinds, W. C. (1999). *Aerosol Technol.: Properties, Behavior, and Measurement of Airborne Particles*, John Wiley and Sons, New York.
- Hood, E. (2004). Nanotechnology: Looking as We Leap. *Environ. Health Perspect.* 112(13):A740–749.
- Jaques, P. A., and Kim, C. S. (2000). Measurement of Total Lung Deposition of Inhaled Ultrafine Particles in Healthy Men and Women. *Inhal. Toxicol.* 12(8):715–731.
- Kittelson, D. B. (1998). Engines and Nanoparticles: A Review. *J. Aerosol Sci.* 29(5–6):575–588.
- Kousaka, Y., Niida, T., Okuyama, K., and Tanaka, H. (1982). Development of a Mixing Type Condensation Nucleus Counter. *J. Aerosol Sci.* 13(3):231–240.
- Kreyling, W. G., Semmler-Behnke, M., and Moller, W. (2006). Ultrafine Particle-Lung Interactions: Does Size Matter? *J. Aerosol Med.* 19:74–83.
- Kreyling, W. G., Semmler, M., and Moller, W. (2004). Dosimetry and Toxicology of Ultrafine Particles. *J. Aerosol Med.* 17(2):140–152.
- Larsson, A., Gustafsson, A., and Svanbord, L. (2000). A New Device for 100% Humidification of Inspired Air. *Critical Care.* 4:54–60.
- Leach, C. L., Davidson, P. J., and Bouhuys, A. (1998). Improved Airway Targeting with the CFC-Free HFA-Beclomethasone Metered-Dose Inhaler Compared with CFC-Beclomethasone. *Euro. Respir. J.* 12:1346–1353.
- Longest, P. W., Hindle, M., Das Choudhuri, S., and Byron, P. R. (2008). Developing a Better Understanding of Spray System Design using a Combination of CFD Modeling and Experiment, in *Proceedings of Respiratory Drug Delivery*, R. N. Dalby, P. R. Byron, J. Peart, J. D. Suman, S. J. Farr, and P. M. Young, eds., Davis Healthcare International, River Grove, IL, pp. 151–163.
- Longest, P. W., Hindle, M., and Xi, J. (2009). Effective Delivery of Nanoparticles and Micrometer-Sized Pharmaceutical Aerosols to the Lung Through Enhanced Condensational Growth, *International Patent Application PCT/US2009/034360*.
- Longest, P. W., and Kleinstreuer, C. (2005). Computational Models for Simulating Multicomponent Aerosol Evaporation in the Upper Respiratory Airways. *Aerosol Sci. Technol.* 39:124–138.
- Longest, P. W., and Xi, J. (2008). Condensational Growth May Contribute to the Enhanced Deposition of Cigarette Smoke Particles in the Upper Respiratory Tract. *Aerosol Sci. Technol.* 42:579–602.
- Lui, B. Y. H., McMurry, P. H., and Sun, J. (1993). Condensation-Growth Particle Scrubber. *U.S. Patent Number 5,176,723*.
- Mandell, G. L., Bennett, J. E., and Bolin, R. D. (2004). *Principles and Practices of Infectious Diseases*. Churchill Livingstone, New York.
- Maynard, A. D., Baron, P. A., Foley, M., Shvedova, A. A., Kisin, E. R., and Castanova, V. (2004). Exposure to Carbon Nanotube Material: Aerosol Release During the Handling of Unrefined Single Walled Carbon Nanotube Material. *J. Toxicol. Environ. Health, Part A.* 67:87–107.
- Maze, B., Tafreshi, H. V., Wang, Q., and Pourdeyhimi, B. (2007). A Simulation of Unsteady-State Filtration via Nanofiber Media at Reduced Operating Pressures. *J. Aerosol Sci.* 38:550–571.
- McMurry, P. H. (2000). The History of Condensation Nucleus Counters. *Aerosol Sci. Technol.* 33:297–322.
- Morawska, L., Hofmann, W., Hitchins-Loveday, J., Swanson, C., and Mengersen, K. (2005). Experimental Study of the Deposition of Combustion Aerosols in the Human Respiratory Tract. *J. Aerosol Sci.* 36:939–957.
- Mordas, G., Sipila, M., and Kulmala, M. (2008). Nanometer Particle Detection by the Condensation Particle Counter UF-02proto. *Aerosol Sci. Technol.* 42:521–527.
- Oberdorster, G., Sharp, Z., Atudorei, V., Elder, A., Gelein, R., Kreyling, W., and Cox, C. (2004). Translocation of Inhaled Ultrafine Particles to the Brain. *Inhal. Toxicol.* 16(6–7):437–445.
- Petaja, T., Mordas, G., Manninen, H., Aalto, P. P., Hameri, K., and Kulmala, M. (2006). Detection Efficiency of Water-Based TSI Condensation Particle Counter 3785. *Aerosol Sci. Technol.* 40:1090–1097.
- Pollak, L. W. (1959). Counting of Aitken Nuclei and Applications of the Counting Results. *Int. J. Air Pollut.* 1:293–306.
- Sioutas, C., and Koutrakis, P. (1996). Inertial Separation of Ultrafine Particles Using a Condensational Growth/Virtual Impaction System. *Aerosol Sci. Technol.* 25(4):424–436.
- Smaldone, G. C. (2006). Advances in Aerosols: Adult Respiratory Disease. *J. Aerosol Med.* 19(1):36–46.

- Stahlhofen, W., Rudolf, G., and James, A. C. (1989). Intercomparison of Experimental Regional Aerosol Deposition Data. *J. Aerosol Med.* 2(3):285–308.
- Stolzenburg, M. R., and McMurry, P. H. (1991). An Ultrafine Aerosol Condensation Nucleus Counter. *Aerosol Sci. Technol.* 14:48–65.
- Sun, J., Lui, B. Y. H., McMurry, P. H., and Greenwood, S. A. (1994). A Method to Increase Control Efficiencies of Wet Scrubber for Submicron Particles and Particulate Metals. *Air and Waste.* 44:184–185.
- Tepper, G., and Kessick, R. (2008). A Study of Ionization and Collection Efficiencies in Electrospray-Based Electrostatic Precipitators. *Aerosol Sci.* 39:609–617.
- Wang, J., McNeill, V. F., Collins, D. R., and Flagan, R. C. (2002). Fast Mixing Condensation Nucleus Counter: Application to Rapid Scanning Differential Mobility Analyzer Measurements. *Aerosol Sci. Technol.* 36:678–689.
- Xi, J., and Longest, P. W. (2008a). Effects of Oral Airway Geometry Characteristics on the Diffusional Deposition of Inhaled Nanoparticles. *ASME J. Biomechanical Engineering.* 130:011008.
- Xi, J., and Longest, P. W. (2008b). Numerical Predictions of Submicrometer Aerosol Deposition in the Nasal Cavity using a Novel Drift Flux Approach. *Intl. J. Heat & Mass Transfer.* 51:5562–5577.